GALCIT REPORT NO. 221-B
INCLUDING APPENDIX I

COPY 1 of 3

GUGGENHEIM AERONAUTICS LABORATORY

CALIFORNIA INSTITUTE OF TECHNOLOGY

WIND TUNNEL TESTS ~~ON MODIFICATIONS TO~~ OF THE "MODERNIZED" XPB2Y-1 MODEL (PB2Y-2)

REPORT 221-B

CONFIDENTIAL

GUGGENHEIM AERONAUTICS LABORATORY

CALIFORNIA INSTITUTE OF TECHNOLOGY

PASADENA

REPORT ON

WIND TUNNEL TESTS ~~ON MODIFICATIONS TO~~ OF THE "MODERNIZED" XPB2Y-1 MODEL (PB2Y-2)

PREPARED BY

Clark B. Millikan

No. of pages 29

No. of figures 12

No. of photographs 13

Date March 7, 1939

Wind Tunnel Section

INDEX OF RUNS

Run	Configuration	Test	q gm/cm2	Settings (degrees)	Fig. No. Ref.
1	Tare C_y on rigging strut	Y	35		
2	$W_1B_7PN_5$	"	"	i = 3, α_u = 3	9
3	$W_1B_7PN_5M_5$	"	"	" , "	"
4	$W_1B_7PN_5H_{18}$	"	"	" , " , s = -1	"
5	$W_1B_7PN_5M_5H_{18}$	"	"	" , " , "	"
6	$W_1B_7PN_5H_{18}V_{11}$	"	"	" , " , " , r = 0	"
7	$W_1B_7PN_5M_5H_{18}V_{11}$	"	"	" , " , " , "	"
8	$W_1B_7PN_5M_5H_{18}V_{12}$	"	"	" , " , " , "	9,11
9	$W_1B_7PN_5H_{18}V_{12}$	"	"	" , " , " , "	9,11
10	$W_1B_7PN_5M_{10}H_{18}V_{12}$	"	"	" , " , " , "	11
11	$W_1B_7PN_5M_8H_{18}V_{12}$	"	"	" , " , " , "	"
12	$W_1B_7PN_5M_9H_{18}V_{12}$	"	"	" , " , " , "	"
13	$W_1B_7PN_5M_5M_6K_2H_{18}V_{12}$	"	"	" , " , " , "	"
14	$W_1B_7PN_5M_5H_{18}V_{13}$	"	"	" , " , " , "	9
15	$W_1B_7PN_5H_{18}V_{13}$	"	"	" , " , " , "	"
16	$W_1B_7PN_5H_{18}V_{12}$	HMY	"	" , " , " , ψ = -2.5	12
17	"	"	"	" , " , " , +5	"
18	"	"	"	" , " , " , +2.5	"
19	"	"	"	" , " , " , 0	"
20	"	"	"	" , " , " , -5	"
21	"	"	"	" , " , " , -10	"
22	"	"	"	" , " , " , -15	"
23	W_1B_7P	mDP	"	"	6,7
24	$W_1B_7PN_5$	"	"	"	6,7
25	$W_1B_7PN_5H_{18}V_{11}$	"	"	" , s = -1.3, e = 0	6,7
26	$W_1B_7PN_5H_{18}V_{12}$	"	"	" , " , "	6,7,8

INDEX OF RUNS

Run	Configuration	Test	q	Settings (degrees)	Fig. No. Ref.
27	$W_1B_7PN_5M_9H_{18}V_{12}$	mD	35	i = 3, s = -1.3, e = 0	8
28	$W_1B_7PN_5M_{10}H_{18}V_{12}$	MD	"	" , " , "	"
29	$W_1B_7PN_5M_5H_{18}V_{12}$	mDP	"	" , " , "	6,8
30	$W_1B_7PN_5M_5K_2H_{18}V_{12}$	MD	"	" , " , "	8
31	$W_1B_7PN_5M_5M_6K_2H_{18}V_{12}$	"	"	" , " , "	"

Definition of Tests:

Y = Yawing moments at angles of yaw

H.M. = Hinge moments

mD = Short minimum drag Run

MD = Complete " " "

P = Complete polar

INDEX OF FIGURES

1. Three-view of the Consolidated "Modernized" XPB2Y-1 model
2. Sketch showing nacelles, N_5
3. Turrets and dome for "modernized" XPB2Y-1
4. Sketch of vertical tail surfaces V_{12}
5. Sketch of vertical tail surfaces V_{13}

Three-Component and Parasite-Drag Measurements

6. Effect of nacelles, tail surfaces, and turret M_5 - three-component data
7. " " " , " " , " " " - parasite drag
8. Effect of turrets and dome - parasite drag

Yawing Moments at Angles of Yaw, Rudder Effectiveness and Hinge Moments

9. Effect of tail surfaces and turret M_5 - yaw at yaw
10. Tail yawing moments for V_{11}, V_{12}, V_{13}
11. Effect of turrets and dome - yaw at yaw
12. Yawing and rudder hinge moment vs. rudder deflection at various angles of yaw

INDEX OF PHOTOS

1. $W_1B_7PN_5H_{18}V_{11}$
2. $W_1B_7PN_5H_{18}V_{12}$
3. 3/4 front view showing N_5
4. Side view showing M_5, M_6, and K_2
5. Rigging strut setup (yaw)
6. $W_1B_7PN_5M_5H_{18}$ (yaw)
7. 3/4 rear view of H_{18} and yaw-rigging strut
8. Bottom view of $H_{18}V_{11}$
9. Top view of $H_{18}V_{11}$
10. 3/4 rear view showing M_5, M_6, and K_2
11. Rear view showing $H_{18}V_{13}$
12. Hinge-moment setup on V_{12}
13. " " " " "

TABLE 1

Notation Used to Describe Configurations Tested

		Consolidated Dwg. No.	Fig. No.	Photo No.
W_1 =	wing of GALCIT Rep. 221-A			
B_7 =	hull B_3 of GALCIT Rep. 221-A refinished and hull lines checked with original drawings	29Z018		1,2
P =	wing tip floats of GALCIT Reps. 221 and 221-A			
N_5 =	nacelles of GALCIT Rep. 221-A with nose opening filled with wood instead of wax	29Z007	2	3
M_5 =	gun turret of Rep. 221-A	29Z015		4,10
M_6 =	retractable side turrets of Rep. 221-A	29Z014		4,10
M_8 =	top gun turret	29Z200	3	
M_9 =	" " "	29Z201	"	
M_{10} =	" " "	29Z042	"	
K_2 =	hemispherical navigator's dome	29Z202	"	4,10
H_{18} =	complete horizontal tail, H_{18}, of GALCIT Rep. 221			
V_{11} =	complete vertical tails, V_{11}, of GALCIT Rep. 221			1
V_{12} =	complete vertical tail surfaces	29Z012	4	2
V_{13} =	" " " "	29Z008	5	11
α_u =	angle of attack relative to root chord, uncorrected for wind tunnel wall interference			
α =	angle of attack relative to root chord, corrected for wind tunnel wall interference			
i =	angle of incidence of the wing = 3^o			
s =	stabilizer angle relative to root chord			
e =	elevator angle relative to stabilizer			
ψ =	angle of yaw relative to plane of symmetry			
q =	dynamic pressure $(\rho/2)V^2$ in gm./cm.^{2}			

REPORT ON
WIND TUNNEL TESTS ON MODIFICATIONS TO
THE "MODERNIZED" XPB2Y-1 MODEL

I. Introduction; General Description of Model and Tests

This Report, to be considered as supplementary to GALCIT Reports 221 and 221-A, describes the results of wind tunnel tests on the "Modernized" version of the model discussed in the earlier Reports. The elements modified were the hull (including gun turrets and navigator's dome), vertical surfaces, and nacelles. Three-component data were obtained as well as yawing moments at angles of yaw. The testing technique, method of reduction and presentation of data, etc., were the same as in the previous Reports and will not be further discussed here.

A three-view of the full-scale airplane is given in Fig. 1, the nacelle appears in Fig. 2, the turrets and dome are shown in Fig. 3, and the vertical surfaces in Figs. 4 and 5. The notation used to describe the various configurations tested is listed in Table 1. The dimensions, assumed C.G. location, etc., used in reducing the data are the same as for the appropriate cases of Report 221 and are not repeated here. The special yaw rigging is that discussed in Report 221-A, Section II,2.

The results are discussed in Section II under the following headings:

1) Three-component and parasite-drag measurements

2) Yawing moments at angles of yaw, rudder effectiveness and hinge moment.

II. Experimental Results and Discussion

1) Three-Component and Parasite-Drag Measurements (Figs. 6-8)

Fig. 6 presents three-component data giving the effect of adding nacelles, tail surfaces, and gun turret M_5 to the wing-hull-tip float configuration. Certain comparative results from Report 221-A are also included. With only wing, hull, and tip floats, the data from the two Reports are in excellent agreement, except that the present tests give a slightly higher stalling angle and a correspondingly higher $C_{L_{max}}$. With the addition of nacelles, N_5, however, a disagreement appears. Up to $\alpha \doteq 13^\circ$ the old and new results are practically indistinguishable. At this attitude the results of the present investigation indicate a premature stall which, as the balance readings show, is accompanied by a large change in rolling moment. This abnormal rolling moment persists until approximately $\alpha \doteq 16.1^\circ$, where it disappears. It therefore seems that the premature stall is actually a stall of one side of the wing induced by the nacelles on that side. At $\alpha \doteq 16.1^\circ$ the other side of the wing is apparently also stalled, and the abnormal rolling moment then vanishes. The method of attaching nacelles employed with this model makes it difficult to align the nacelles accurately in yaw. It therefore is possible that one of the nacelles was set at an appreciable angle of yaw which might easily induce a premature stall over the wing adjacent to it. If this explanation, or one like it, is correct, then the premature stall is essentially a model characteristic and should not occur on the full-size airplane. It is believed that this is actually the case, and it is accordingly recommended that no attention be paid to the premature stall which appears on all subsequent Runs near $C_{L_{max}}$.

With tail surfaces $H_{18}V_{11}$, the results from the two Reports are nearly identical except for the region near $C_{L_{max}}$, and for a difference in trim. There is a nearly constant difference in C_M of the order of 0.030 between the pertinent curves for the two Reports. With the stabilizer effectiveness found in Report 221-A ($-\frac{dC_M}{ds^o} \doteq 0.030$), about half of this difference is explained by the $1/2^o$ difference in stabilizer setting for the two curves, leaving an unexplained discrepancy corresponding to about $1/2^o$ stabilizer displacement. The accuracy with which a stabilizer setting can be duplicated when the model is removed from the tunnel, disassembled, and reassembled is not much better than $1/4^o$ to $1/2^o$, so that it appears that this remaining discrepancy probably corresponds to uncertainties in the exact stabilizer settings for the two tests in question.

The change from V_{11} to V_{12} and the addition of M_5 produce only negligible effects, as indicated on the small-scale, three-component diagram.

The corresponding parasite-drag results of Fig. 7 show that the configurations of the present Report actually have slightly less drag than the corresponding ones of the earlier Report. Such a difference is not surprising in view of the reworking and smoothing up of the model, which were carried out between the two investigations. The reason for the fact that this difference is somewhat larger with tail surfaces mounted than with them removed is not clear. Fairly small differences in the condition of the tail surfaces, and especially in their fairing to the hull, could account for the phenomenon. If ΔC_{D_p} represents the difference in C_{D_p} between Run 9 of Report 221-A and Run 25 of the present Report, then the increase in ΔC_{D_p} with C_L is explained by the difference in stabilizer

settings. For at about C_L = 0.41 the load on the two tails is practically equal, below this C_L the tail of Report 221-B carries more load than that of Report 221-A, and above this C_L it carries less. Hence the drag due to tail load should be larger for Run 25 (221-B) than for Run 9 (221-A) below $C_L \doteq 0.41$ and smaller above C_L = 0.41. ΔC_{D_p} varies with C_L in exactly the manner that these considerations would suggest.

The parasite drags of V_{11} and V_{12} are nearly indistinguishable even with the large C_{D_p} scale employed in Fig. 7.

Fig. 8 gives parasite-drag data for all of the turrets and domes investigated. All give relatively small drag increments, M_5 and M_9 giving the smallest values, which are practically identical. M_6 and K_2 furnish somewhat larger increments which, again, are nearly equal. M_{10} gives considerably the largest drag of any of the turrets or domes.

Drag-coefficient increments and proper drags have been collected in Table 2 below, where comparative data from Report 221-A are also included.

TABLE 2

Drag-Coefficient Increments and Proper Drags

Item	C_L	ΔC_{D_p} based on area = 8440 cm.^{2}		S_π (cm.^{2})	Proper Drag Coef., C_{D_π}	Proper Drag Coef., C_{D_π} From Rep. 221-A
		Rep. 221-B	Rep. 221-A			
Nacelles, N_5	0.3	0.0023	0.0025	290.0	0.067	0.073
Turret, M_5	"	0.0002	0.0002	--	--	--
Turret, M_6	"	0.0004	0.0003	--	--	--
Turret, M_9	"	0.0002	--	--	--	--
Turret, M_{10}	"	0.0008	--	--	--	--
Tail Surfaces $H_{18}V_{11}$, $s = -1.3$	0.47	0.0031	0.0035 ($s = -0.85°$) ($C_L = 0.35$)	2400	0.0109	0.0123
Tail Surfaces $H_{18}V_{12}$, $s = -1.3$	"	0.0032	--	2525	0.0107	--

The agreement between the two Reports is satisfactory, the nacelle and tail-surface drags being a little lower in the present Report than in Report 221-A.

Note: In the original form of Report 221-A, an erroneous, excessively large drag was given for M_6. This was corrected to the value given above at the time of the present investigation when the original error was discovered (cf. corrected p. 6 and Fig. 8 of Rep. 221-A).

2) Yawing Moment at Angles of Yaw, Rudder Effectiveness and Hinge Moment (Figs. 9-12)

Yawing moment at angles of yaw is presented in Fig. 9 for various tail surfaces, with and without turret M_5. Two curves from Report 221-A are also given for configurations comparable to those tested in the present investigation. The agreement between the two Reports is very satisfactory, such small differences as do appear being explainable by the slight changes in the model made between the two investigations. All of the tail configurations were tested with and without turret M_5. In every case the effect of the turret is negligible, being of the order of the experimental scatter. This result is in disagreement with that originally obtained in Report 221-A, Run 17. A check of this Run revealed an error in the data reduction which, when corrected, led to the result that the effect of M_5 on yawing moment was negligible, as shown by the corrected data of Report 221-A (cf. corrected Fig. 15 of Rep. 221-A).

For all of the tail surface configurations, the directional stability is fairly constant for $-4^\circ \leq \psi \leq +4^\circ$ and again for $10^\circ < |\psi| < 21^\circ$. The results are accordingly tabulated below for these two ranges of yaw angle. For $4^\circ < |\psi| < 10^\circ$ the stability increases continuously from the lower to the higher value.

TABLE 3

Summary of Directional Stabilities

Tail Surfaces	$-dC_y/d\psi^o$	
	$-4^o \leq \psi \leq +4^o$	$10^o < \lvert\psi\rvert < 21^o$
None	-0.0009	-0.0003 (roughly)
H_{18}	-0.0006	+0.0002 (")
$H_{18}V_{11}$	+0.0005	0.0016
$H_{18}V_{12}$	0.0007	0.0018
$H_{18}V_{13}$	0.0009	0.0021

From the curves of Fig. 9 the yawing moment due to vertical surfaces, $\left(\frac{dC_y}{d\psi^o}\right)_v$, may be obtained by subtraction. This has been done and the results plotted in Fig. 10. From these curves a vertical tail efficiency factor η_v may be determined. η_v is defined by the following equation which takes into account the aspect ratio of the vertical surfaces:

$$\left(\frac{dC_y}{d\psi^o}\right)_v = -\eta_v \frac{l_v}{b} \frac{S_v}{S_w} \frac{5.5}{1 + \frac{5.5}{\pi AR_v}} \frac{\pi}{180}$$

Here 5.5 is taken as the slope of the lift curve of the vertical surface airfoil profile for infinite aspect ratio in absolute units. η_v is a measure of the interference effects of wing, hull, nacelles, horizontal tail, etc., on the vertical surfaces.

The calculations for the three vertical surfaces follow:

		V_{11}	V_{12}	V_{13}
AR_v	=	1.27 each	1.51	1.51
S_v	=	180.12 ft.^{2} (both)	207.08 ft.^{2} (both)	237.20 ft.^{2} (both)
S_w	=	1780 ft.^{2}	1780 ft.^{2}	1780 ft.^{2}
b	=	115 ft.	115 ft.	115 ft. (approx.)
ℓ_v	=	46.26 ft.	46.26 ft.	46.26 ft.
$\frac{\ell_v}{b}$	=	0.4022	0.4022	0.4022
$\frac{S_v}{S_w}$	=	0.1012	0.1167	0.1333
$1 + \frac{5.5}{\pi AR_v}$	=	2.377	2.158	2.158
$\frac{5.5}{1 + \frac{5.5}{\pi AR_v}}$	=	2.315	2.550	2.550
$\left(\frac{dC_y}{d\psi^o}\right)_v$	=	$-0.001644\ \eta_v$	$-0.002090\ \eta_v$	$-0.002387\ \eta_v$
$\left(\frac{dC_y}{d\psi^o}\right)_v$	=	-0.001195 (Fig.10)	-0.001335 (Fig.10)	-0.001510 (Fig.10)
η_v	=	0.727	0.639	0.633

Fig. 11 presents directional stability data for all of the turrets and the dome mounted on the hull. None of these items has any appreciable effect on the yawing moments, as would be expected in view of the lack of any possible interference between them and the twin vertical surfaces.

In Fig. 12 are given yawing moments and rudder hinge moments as functions of rudder deflection for various angles of yaw with vertical surfaces V_{12}. A curve of yawing moment vs. angle of yaw for zero rudder deflection is also included. The rudder effectiveness

for constant angle of yaw is approximately constant over a range of rudder angles of about 20° in the neighborhood of $r = 0^\circ$. For rudder deflections greater than 10° or 12°, the effectiveness decreases markedly but remains positive to the largest deflections investigated. The rudder effectiveness is also roughly independent of angle of yaw for angles of yaw less than 5°. For larger angles of yaw it decreases somewhat. In the region of constant effectiveness we have approximately:

$$-\frac{dC_y}{dr^\circ} \doteq 0.0009 \quad \left\{ \begin{matrix} -10^\circ \leq r \leq +10^\circ \\ -5^\circ < \psi \leq +5^\circ \end{matrix} \right\} \quad V_{12}$$

The hinge-moment curves indicate considerable underbalance under all conditions and a high degree of stiffness for moderate and large rudder throws. The minimum stiffness is given by

$$\frac{dC_{H_r}}{dr^\circ} \doteq 0.006 \text{ near } \psi = 0^\circ,\ r = 0^\circ$$

For large angles of yaw the stiffness is of the order of five times as large as the above figure.

Conclusion

The investigation described above was carried out from January 19-24, 1939, under the direction of Dr. Clark B. Millikan, who was largely assisted by Messrs. L. B. Rumph, Jr., and W. H. Bowen, and other members of the GALCIT wind tunnnel staff. Messrs. Donald A. Hall and Ernest Stout acted as Consolidated representatives at the tests.

Guggenheim Aeronautics Laboratory
California Institute of Technology
March 7, 1939

CONSOLIDATED
AIRCRAFT CORP.

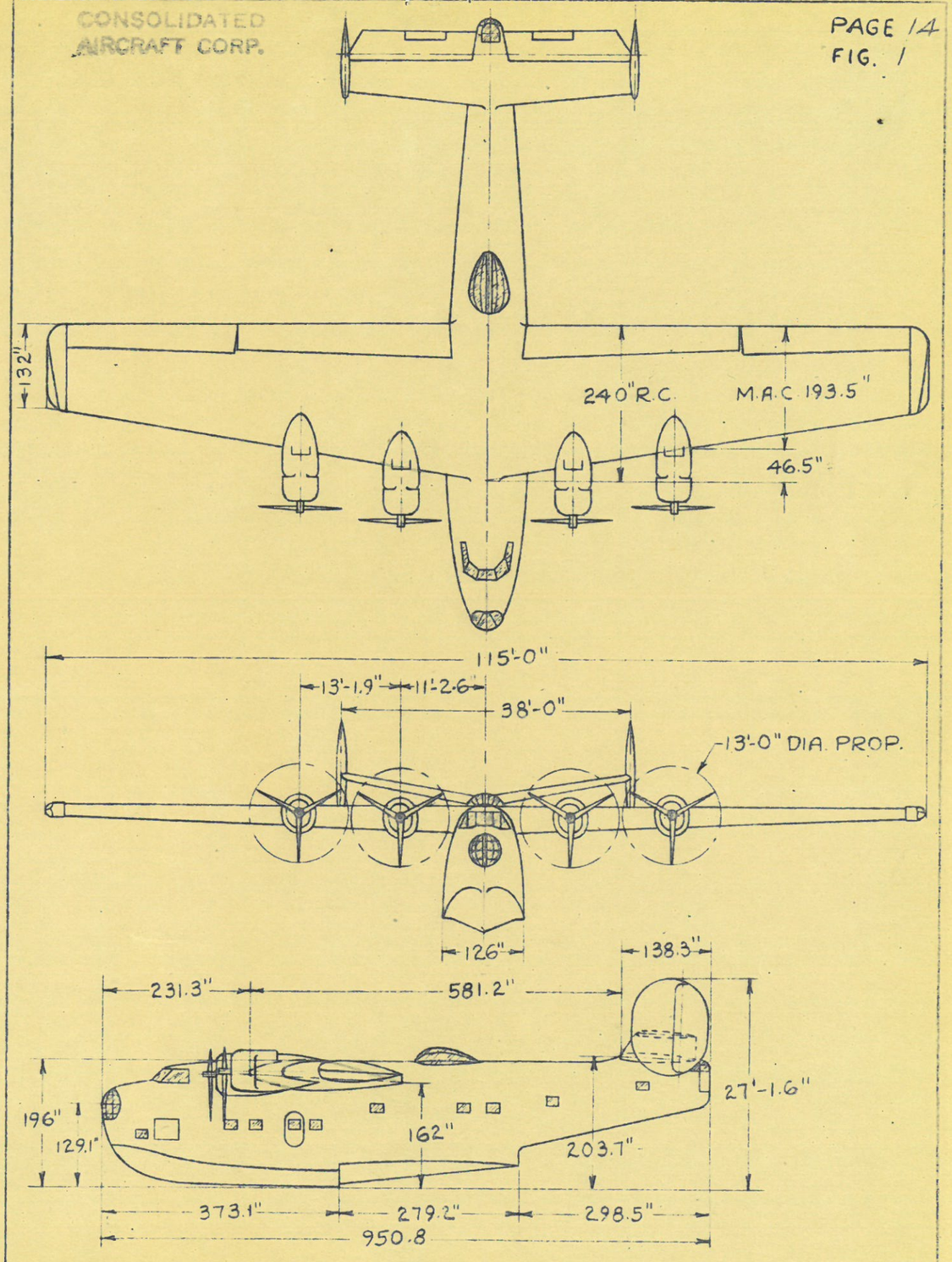

THRUST LINE IS PARALLEL WITH BASE LINE
INCIDENCE OF WING = +3°
NORMAL STAB. = -1° RELATIVE TO WING

XPB2Y-1
MODERNIZED

SCALE 1"=200' [illegible] 1-31-39

GALCIT REP. 221-B

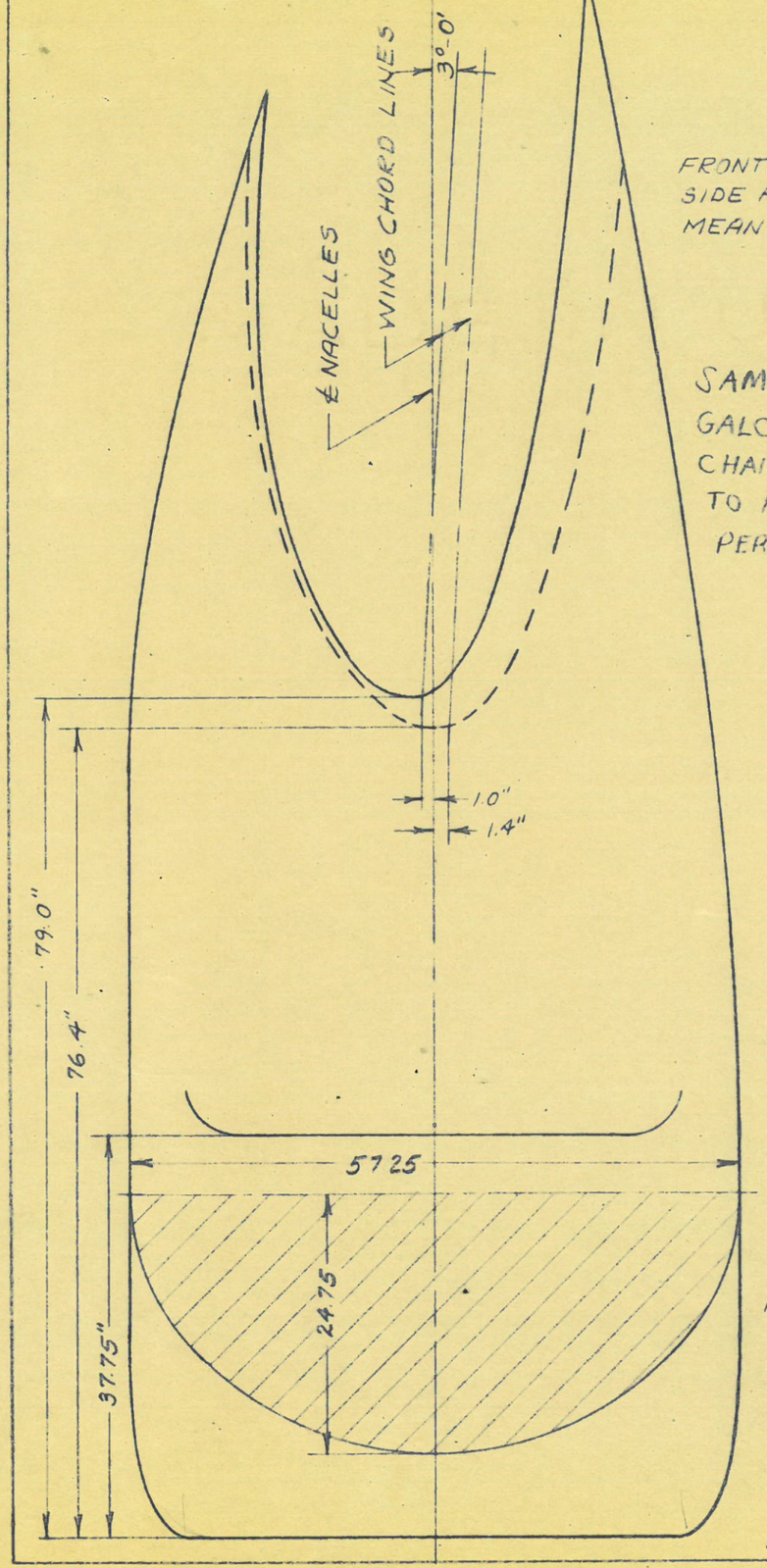

FRONTAL AREA, 15.3 SQ FT.
SIDE AREA FWD OF
MEAN L.E. = 30.6 SQ. FT.

N_5

SAME AS N_5 OF GALCIT 221-A WITH CHANGES FROM N_4 TO N_5 MADE PERMANENT.

REF DRWG
29Z007

N_5 NACELLE
P&W. 1830-76 ENG.
XPB2Y-1
MODERNIZED

SCALE 1"=1'-4"
L.E.M. 1-18-39

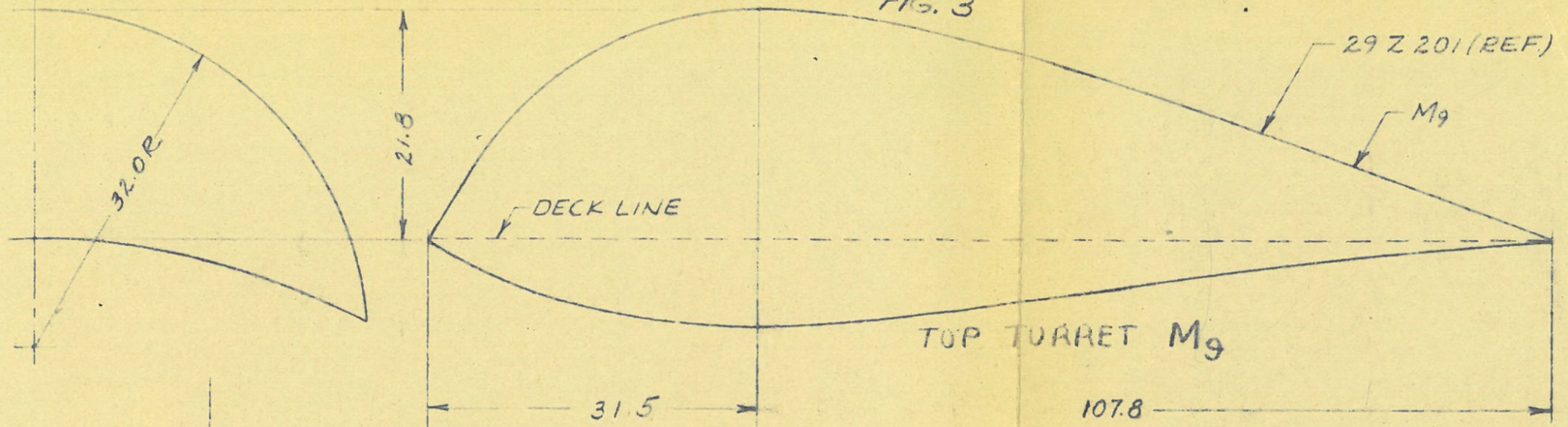

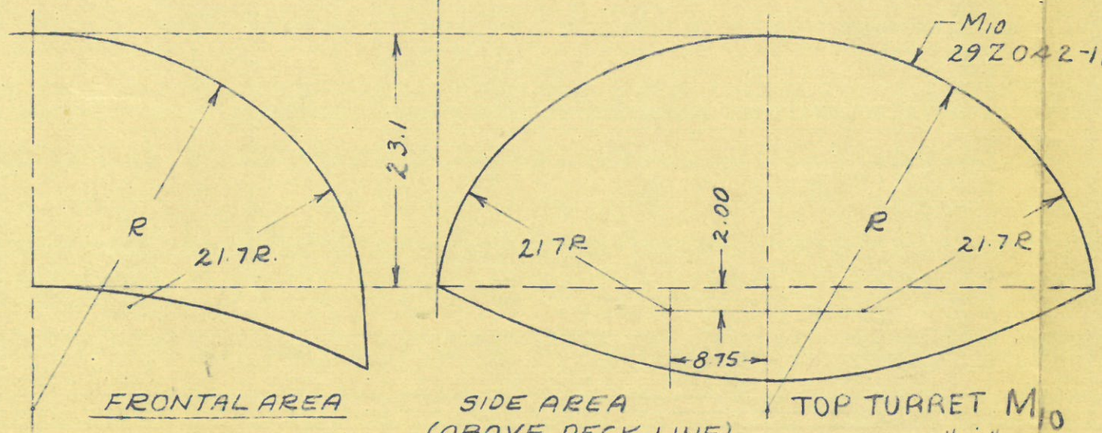

	FRONTAL AREA	SIDE AREA (ABOVE DECK LINE)
M_8	7.70 □'	8.84 □'
M_9	7.70 □'	10.20 □'
M_{10}	8.70 □'	7.55 □'
K_2	1.51 □'	1.57 □'

TOP TURRET M_{10}
SAME AS "M" OF GALCIT 221 FIG. 4
SEE FIG. 26

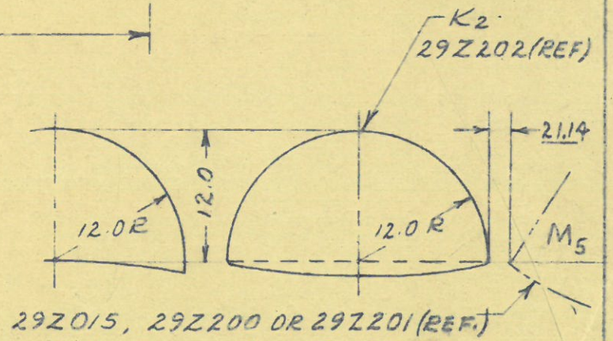

NAVIGATOR'S DOME K_2

TURRETS & DOME XPB2Y-1 MODERNIZED

SCALE 1"=14"

CK. DATA L.E.M. 1-18-39

FORM NO. 154 FRYE & SMITH

GALCIT REP. 221-B

CONSOLIDATED AIRCRAFT CORPORATION

FIG. 4

MODEL XPB2Y-1 AIRPLANE REPORT NO.

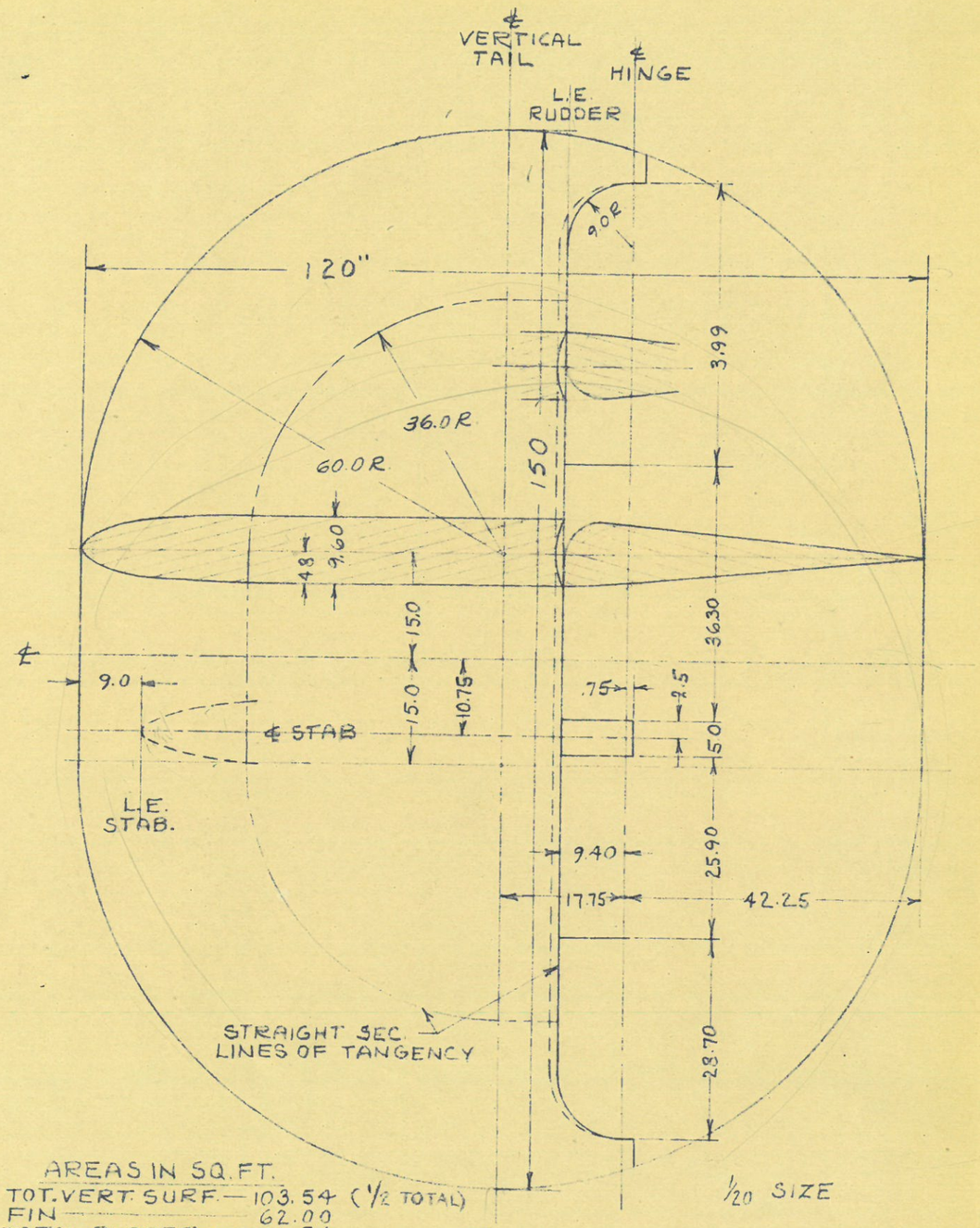

AREAS IN SQ. FT.

TOT. VERT. SURF.	103.54 (½ TOTAL)
FIN	62.00
TOTAL RUDDER	41.54
AFT OF HINGE	33.23
RUDDER BALANCE	8.31
20% BALANCE	

V_{12}

1/20 SIZE

BY L.E.M. 12-15-38

CHECKED

REF. D'W'G. 29Z 012

VERTICAL TAIL #2 (TWIN TAIL)
MODERNIZED XPB2Y-1

FORM NO. 154 FRYE & SMITH

GALCIT REP. 221-B

2.21-B

CONSOLIDATED AIRCRAFT CORPORATION

PAGE 18
FIG. 5

MODEL XPB2Y-1 AIRPLANE REPORT NO.

AREAS IN SQ. FT.

TOTAL VERT. SURF.	118.60 (½)
FIN	74.87
TOTAL RUDDER	43.73
AFT OF HINGE	34.98
RUDDER BALANCE	8.75
20% BALANCE	

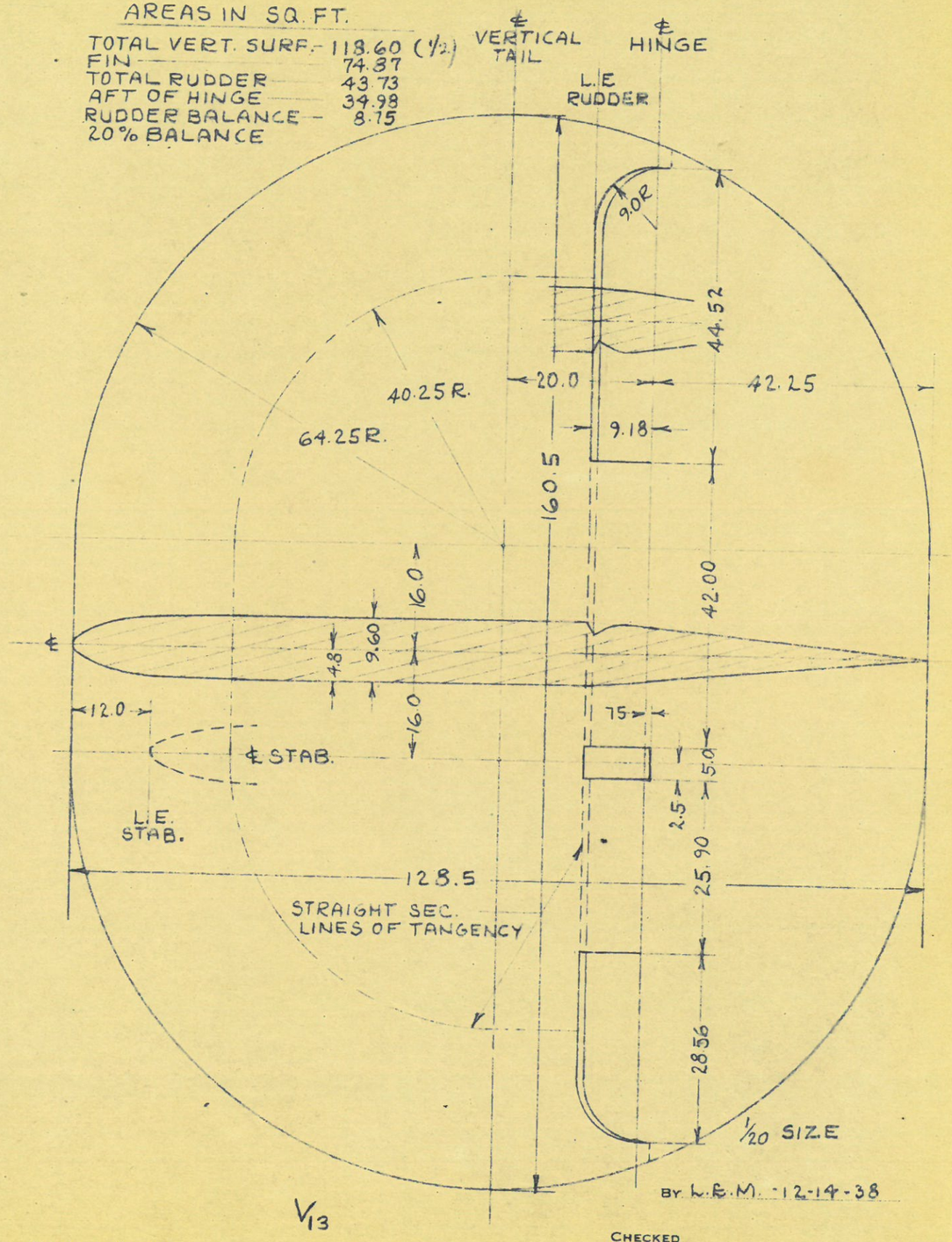

BY L.E.M. 12-14-38

V13

CHECKED

REF. D'W'G. 29Z008

VERTICAL TAIL #3 (TWIN TAIL)
MODERNIZED XPB2Y-1

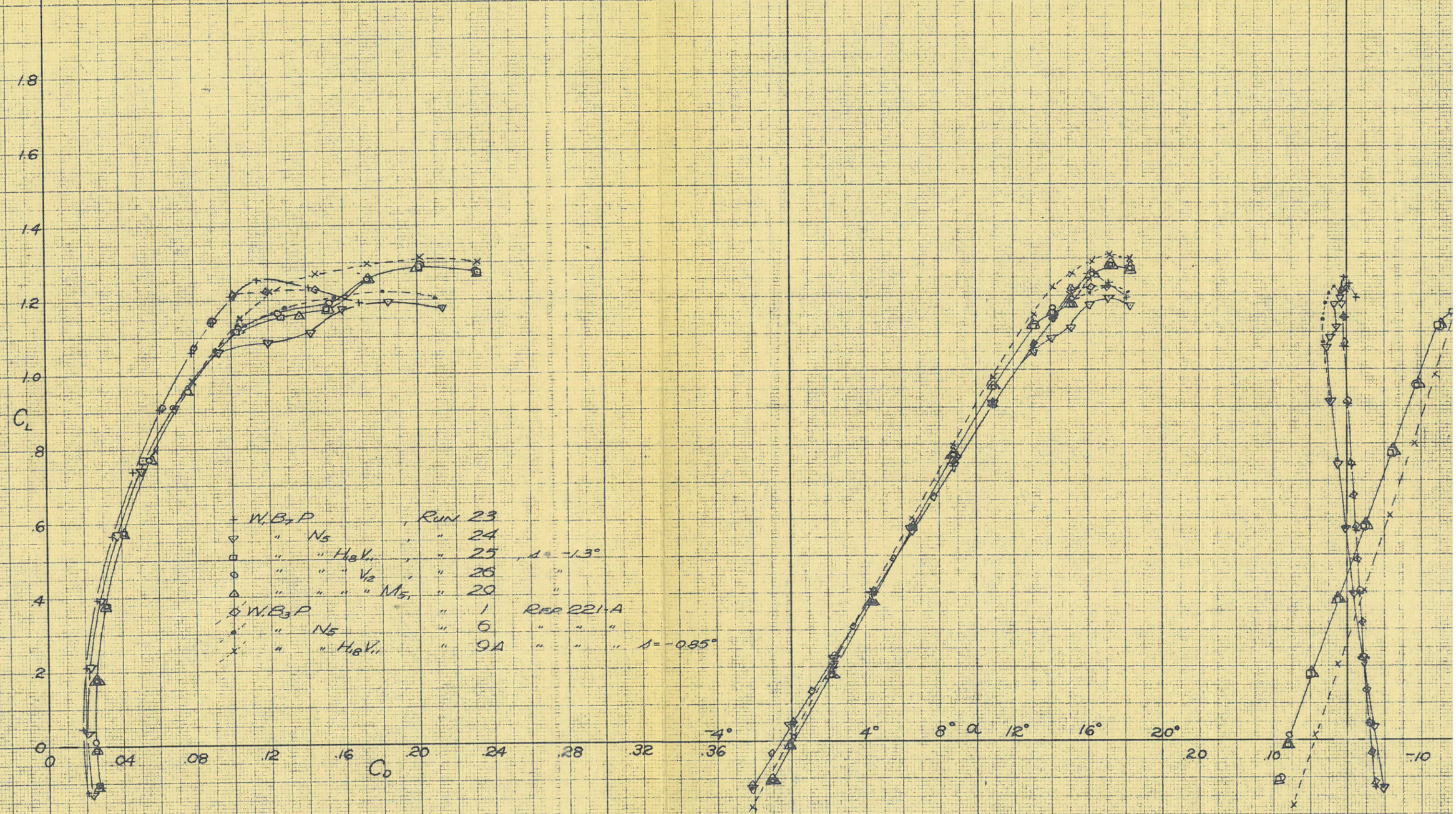

EFFECT OF NACELLES, TAIL SURFACES AND TURRET M$_5$

THREE COMPONENT DATA

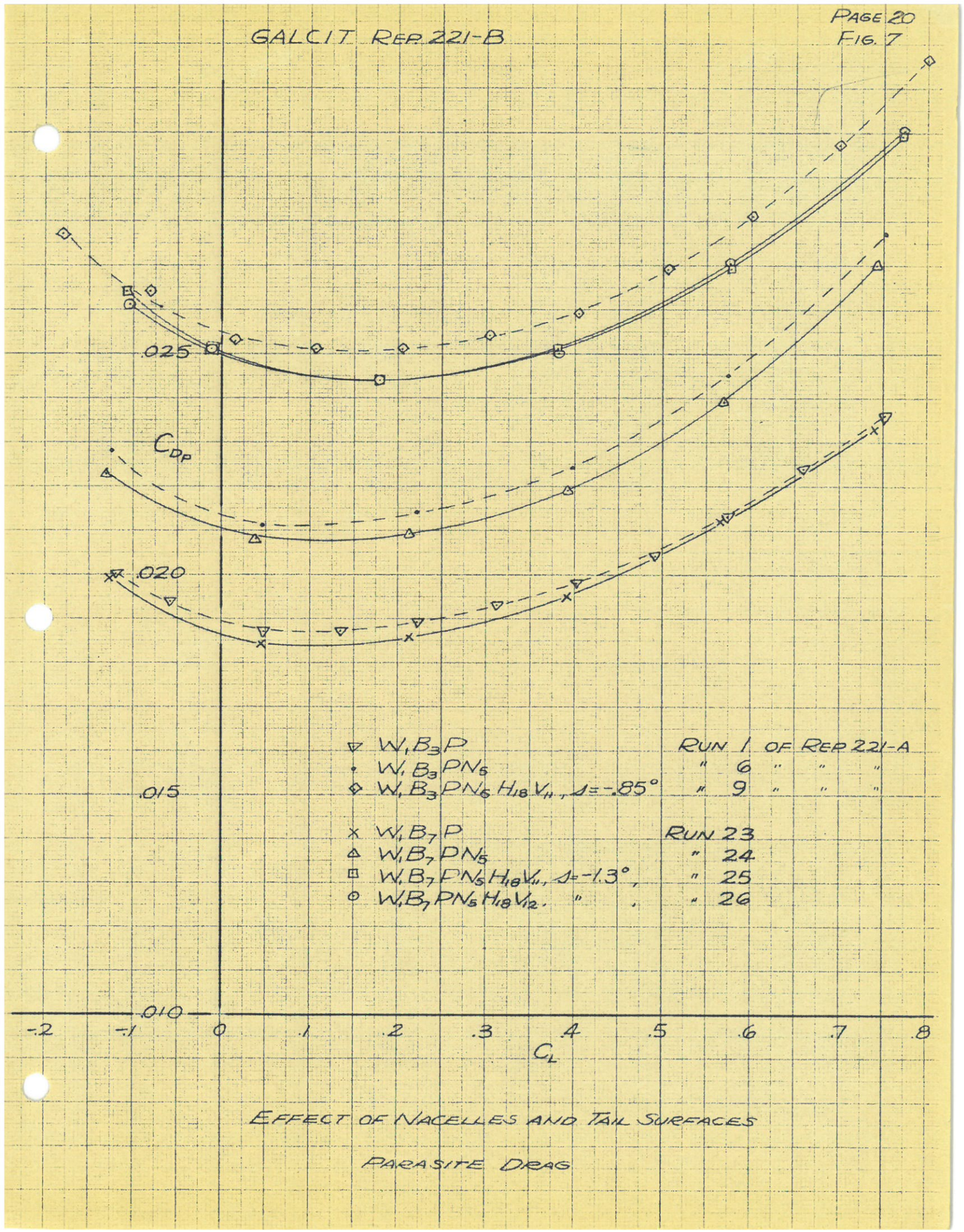

EFFECT OF NACELLES AND TAIL SURFACES

PARASITE DRAG

$\alpha = -1.3°, \epsilon = 0°$

○ $W_1B_2PN_5H_{10}V_{12}$	RUN 26
× $W_1B_2PN_5M_3H_{10}V_{12}$	" 27
□ $W_1B_2PN_5M_{10}H_{10}V_{12}$	" 28
△ $W_1B_2PN_5M_5H_{10}V_{12}$	" 29
▽ $W_1B_2PN_5M_5K_2H_{10}V_{12}$	" 30
+ $W_1B_2PN_5M_5M_6K_2H_{10}V_{12}$	" 31

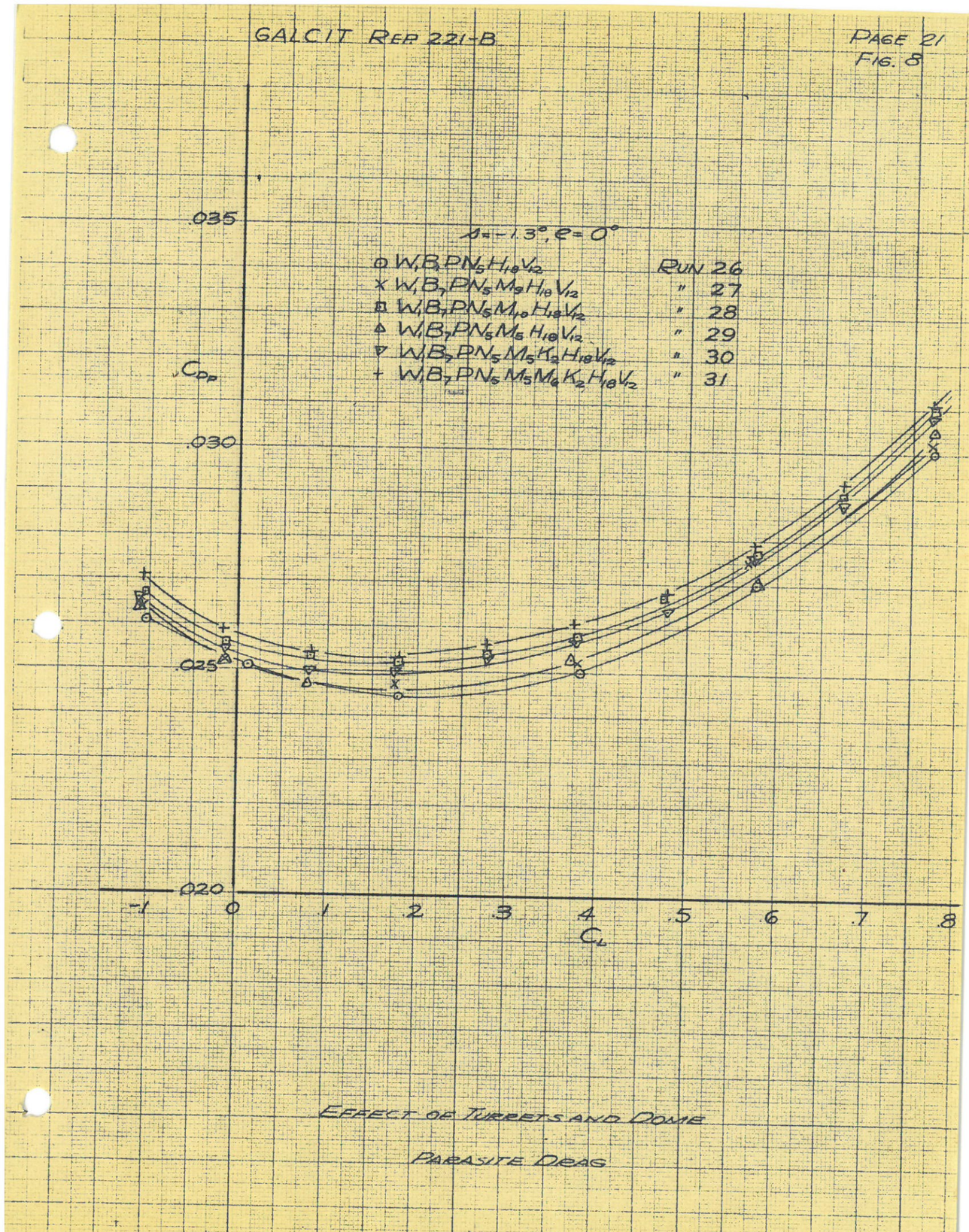

EFFECT OF TURRETS AND DOME

PARASITE DRAG

GALCIT REP 221-B

PAGE 22
FIG 9

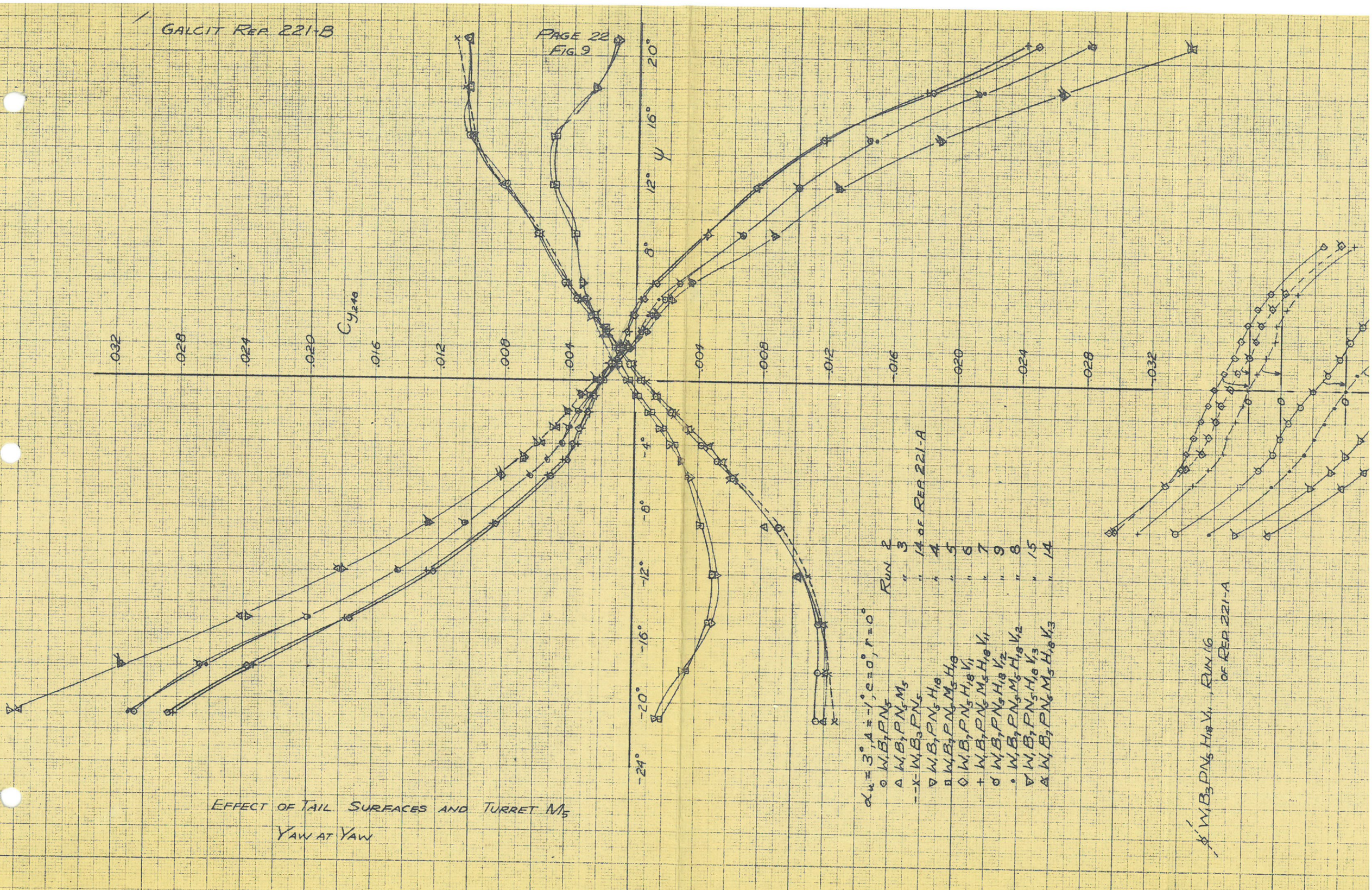

EFFECT OF TAIL SURFACES AND TURRET M_5
YAW AT YAW

C_N

α

20°
16°
12°
8°
4°
0°
-4°
-8°
-12°
-16°
-20°

○ C_N FOR V_{11} (RUN 6) - (RUN 4)
□ " " V_{12} (RUN 9) - "
△ " " V_{13} (RUN 15) - "

TAIL YAWING MOMENTS FOR V_{11}, V_{12}, V_{13}

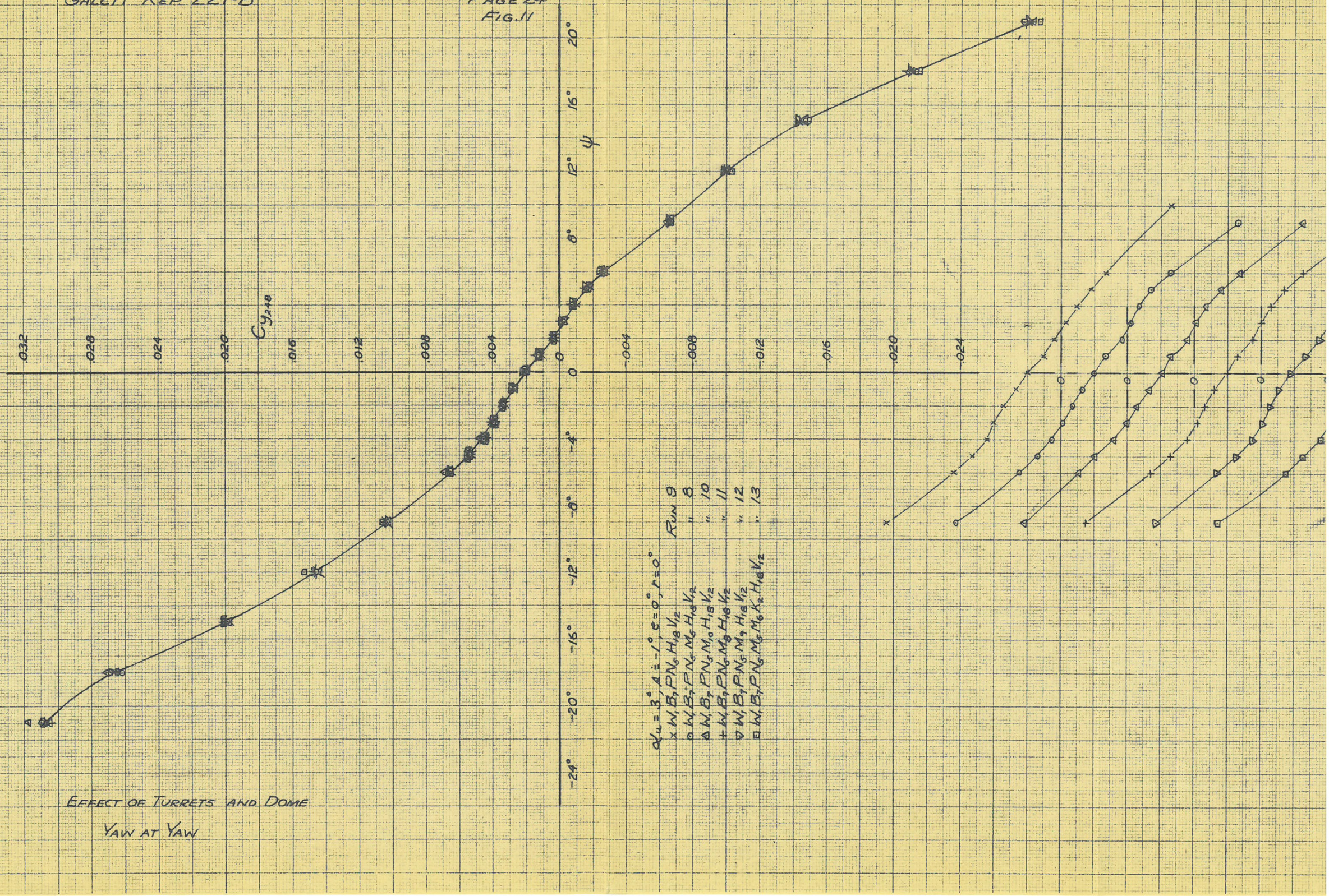

EFFECT OF TURRETS AND DOME

YAW AT YAW

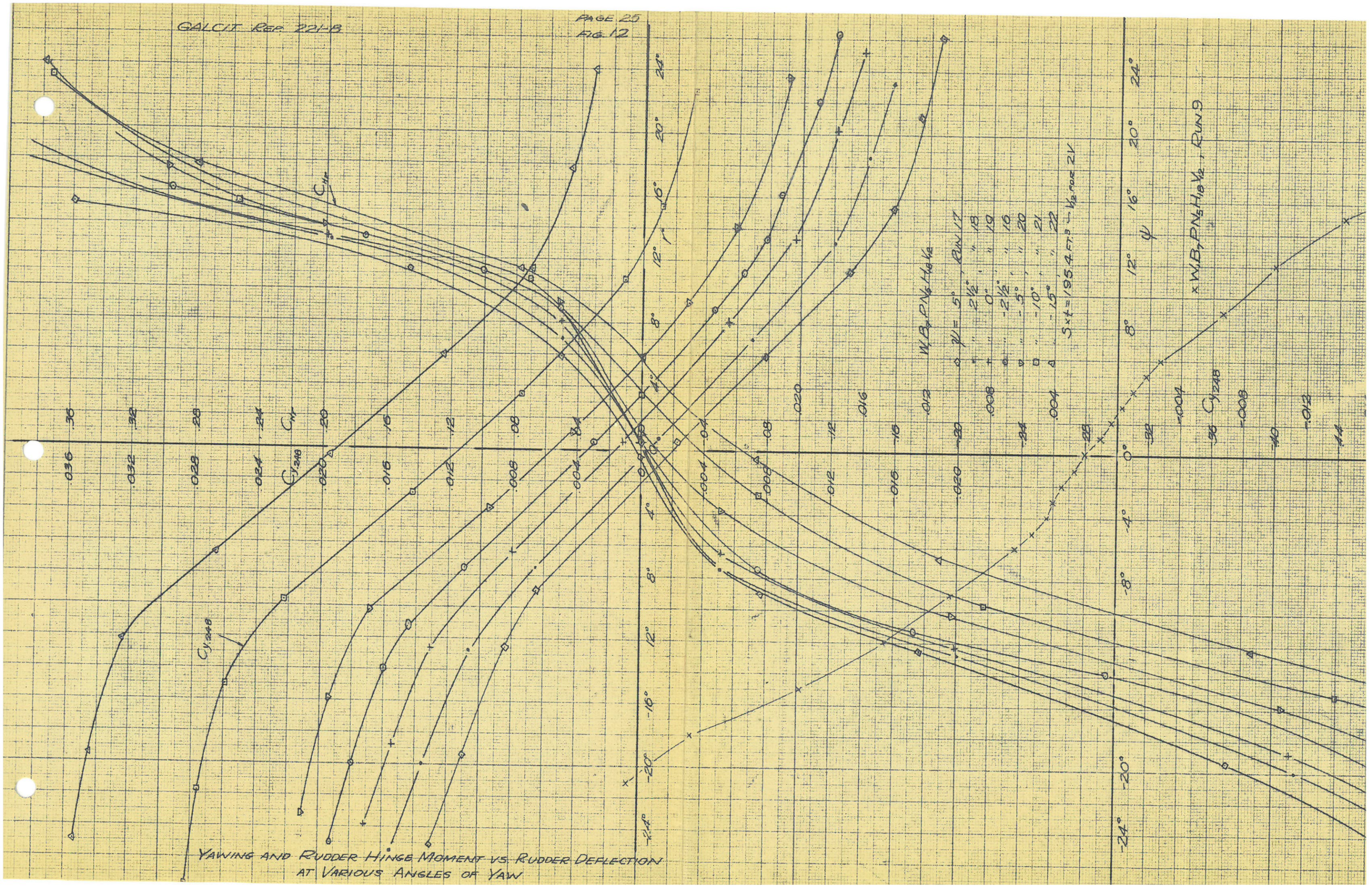

YAWING AND RUDDER HINGE MOMENT VS. RUDDER DEFLECTION AT VARIOUS ANGLES OF YAW

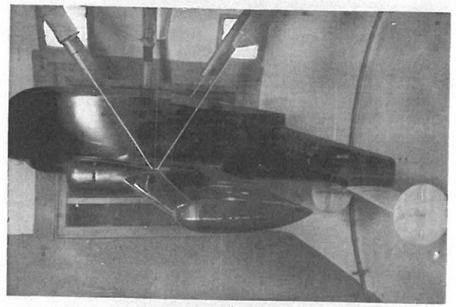

PHOTO 1.
$W_1B_7PN_5H_{18}V_{11}$

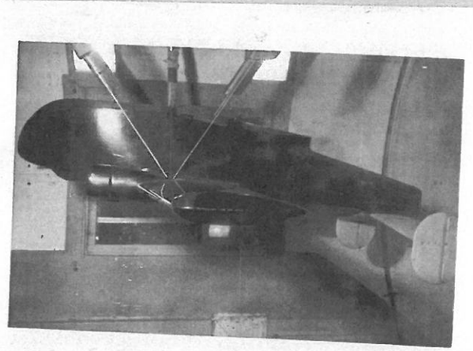

PHOTO 2.
$W_1B_7PN_5H_{18}V_{12}$

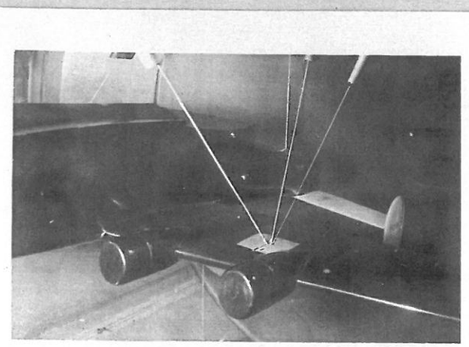

PHOTO 3.
3/4 front view showing N_5

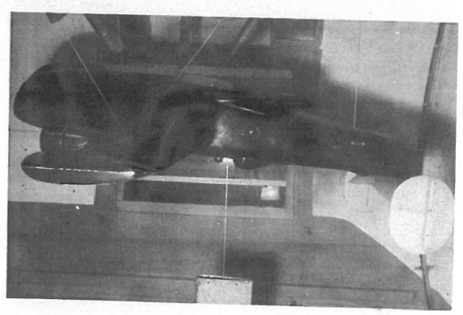

PHOTO 4.
Side view showing M_5, M_6, and K_2

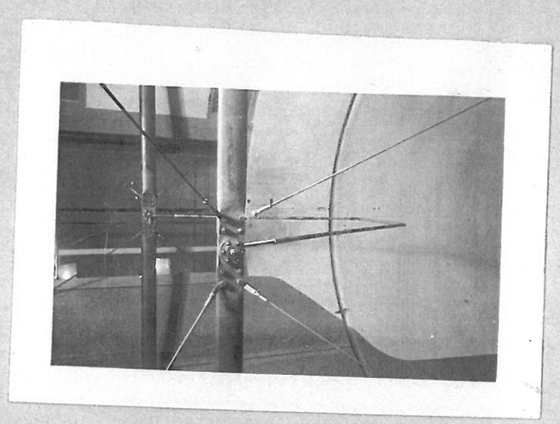

PHOTO 5.
Rigging strut setup (yaw)

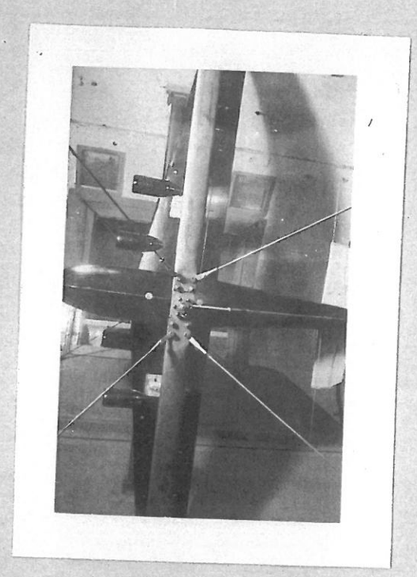

PHOTO 6.
$W_1B_7PN_5M_5H_{18}$ (yaw)

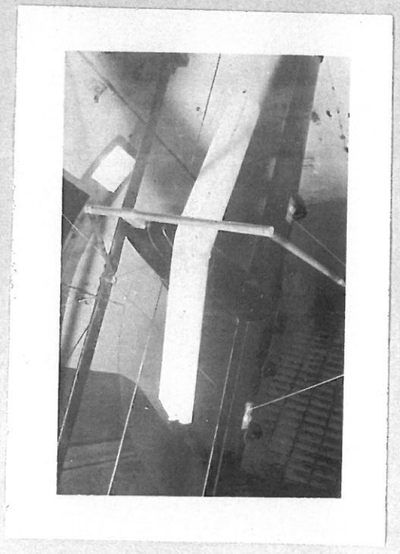

PHOTO 7.
3/4 rear view of H_{18} and
yaw rigging strut

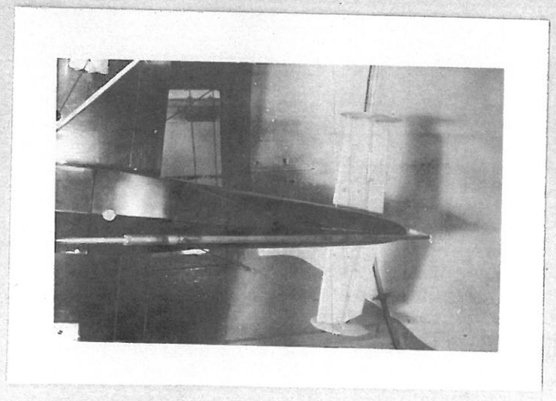

PHOTO 8.
Bottom view of $H_{18}V_{11}$

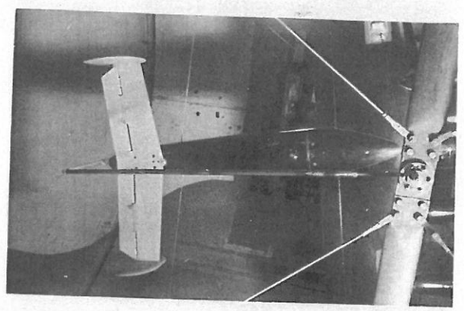

PHOTO 9.
Top view of $H_{18}V_{11}$

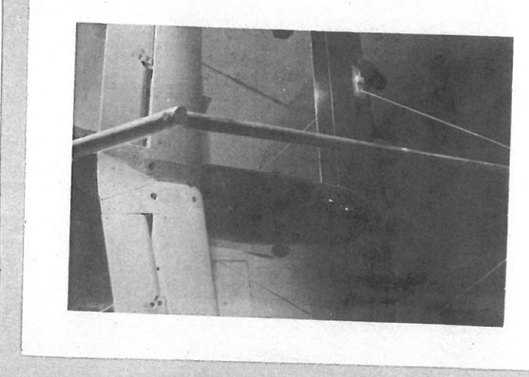

PHOTO 10.
3/4 rear view showing M_5, M_6, and K_2

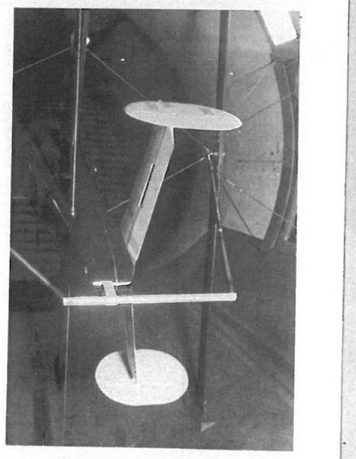

PHOTO 11.
Rear view showing $H_{18}V_{13}$

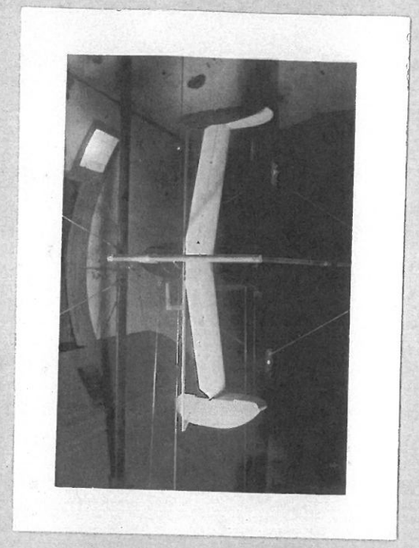

PHOTO 12.
Hinge-moment setup on V_{12}

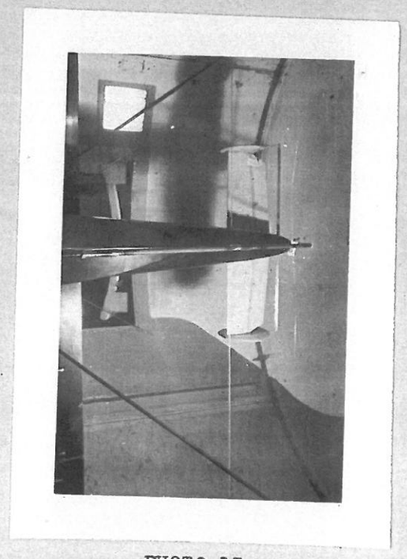

PHOTO 13.
Hinge-moment setup on V_{12}

P29a

CALIFORNIA INSTITUTE OF TECHNOLOGY
PASADENA

DANIEL GUGGENHEIM AERONAUTICAL LABORATORY

March 4, 1939

Mr. H. A. Sutton
Consolidated Aircraft Corporation
San Diego, California

Dear Mr. Sutton:

I am enclosing corrected prints of certain pages in our Report 221-A in which errors have been discovered. Two Runs in this Report (Nos. 11 and 17) gave rather abnormal results. Accordingly, Runs were included in Report 221-B to check them. When the abnormalities were not found in the later Report, a careful check of the earlier Runs was made, and it was discovered that there were errors in the original computations of both Runs. These errors have now been corrected, the corresponding curves replotted, and the pertinent discussions altered in accordance with the corrected results. The sets which I am enclosing are intended to replace the corresponding sheets in the copies of Report 221-A which you already have. The replaced sheets should be destroyed.

I feel very apologetic that I did not catch these errors in my analysis of the tests during the preparation of the Report. When the costs of 221-B are computed, I shall deduct the cost of all Runs which were undertaken with the purpose of checking the abnormal results originally given in 221-A.

I hope very much that the errors did not cause you any difficulty other than that involved in the carrying out of the check Runs of Report 221-B. The latter Report has now been completed and is being typed. It should be sent to you next week.

Very sincerely yours,

Clark B. Millikan

Clark B. Millikan

CBM:MRS
Encls.

APPENDIX 1

About six weeks after the conclusion of the tests described in the body of the Report two additional Runs were made. This appendix discusses the results obtained in these later tests. Run 32 (Fig. 13) was made as a check on Run 26. The premature stall which was discussed on page 7 in connection with Run 26 still remains, although it is less severe with Run 32. It appears that the reason suggested on page 7 is probably correct, namely that small changes in the setting of nacelles N_5 have a pronounced effect on the wing stalling characteristics. Nacelles N_6, identical with N_5 except for a rounding of the nose as indicated in the sketch of Fig. 13, improve the stalling characteristics very appreciably, both with respect to lift and drag. The pitching moments for both Runs 32 and 33 are consistent with the earlier tests of Run 9A, Report 221-A, and indicate that the stabilizer or elevator setting for Run 26 was rather inexact, as suggested on page 8 of the present Report. Both were very carefully checked before Run 32.

Clark B. Millikan

Clark B. Millikan

Guggenheim Aeronautics Laboratory

California Institute of Technology

March 18, 1939

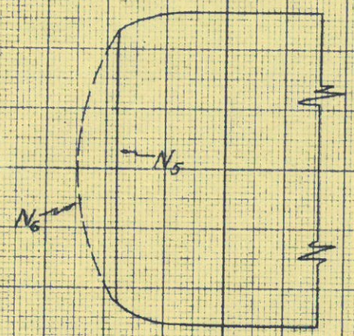

C_L

1.4
1.2
1.0
.8
6
4
.2
0

0 .02 .04 .06 .08 .10 .12 .14 .16 .18

C_D

ϕ W, B, P N_5 H_{18} V_{12} , $i = -1.3°$, $e = 0°$, RUN 26
X " , " , " , " 33
△ W, B, P N_6 H_{18} V_{12} , " , " , " , " 32

-4° 4° 8° 12° 16° 20°

α

.22 .24 20 10° 0 -10

$C_{M_{CG}}$

EFFECT OF NACELLES N_5 AND N_6 ON PREMATURE STALL

3 COMPONENT DATA

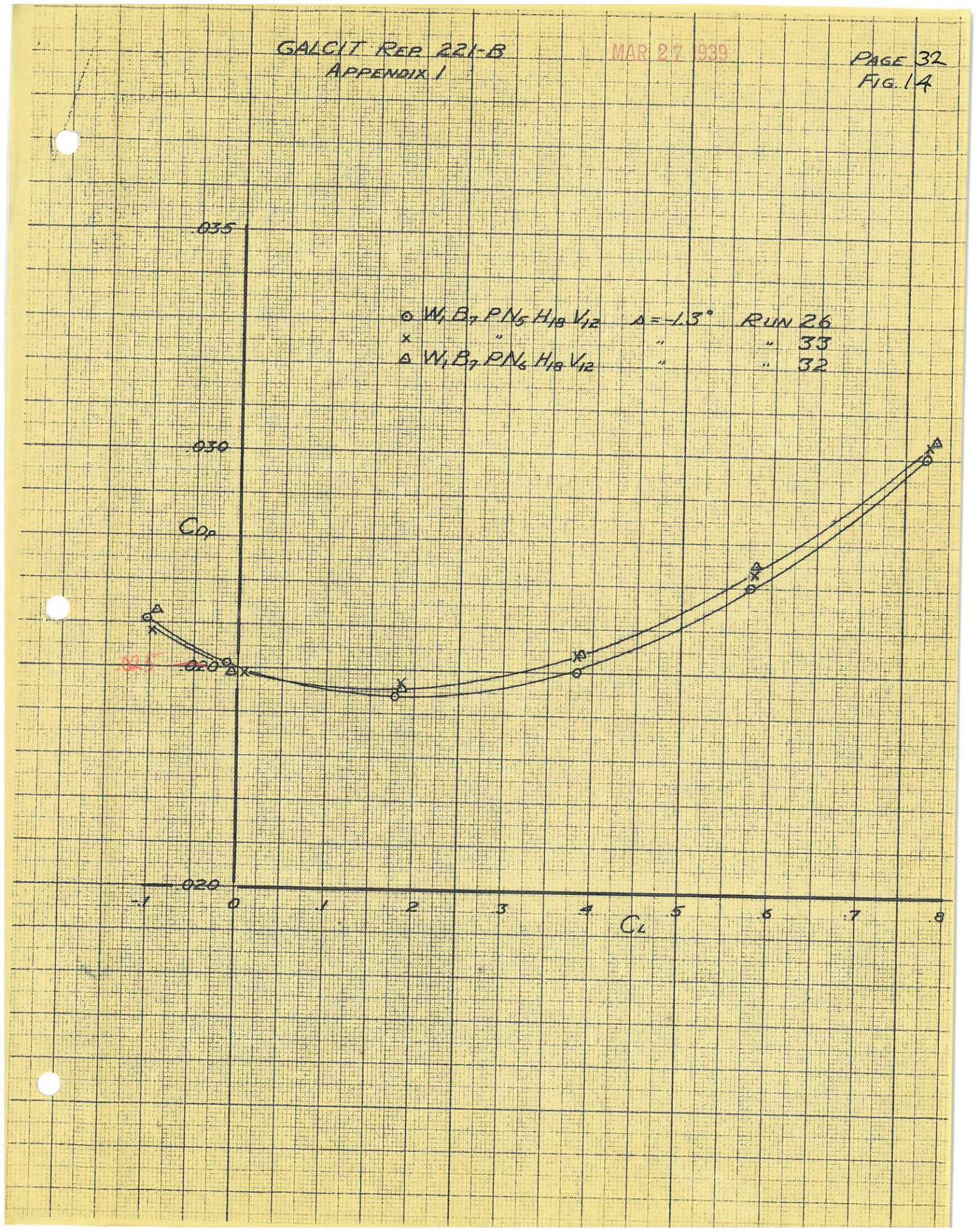
○ $W_1 B_7 P N_5 H_{18} V_{12}$ $\Delta = -1.3°$ RUN 26
× " " " 33
△ $W_1 B_7 P N_6 H_{18} V_{12}$ " " 32
.035
.030
C_{D_P}
.025
.020
-.1
0
.1
.2
.3
.4
C_L
.5
.6
.7
.8